

## Supplementary Information

# Rapid synthesis of hierarchical porous MOFs and the simulation of growth

*Hang Zhang,<sup>†#</sup> Jinhao Huo,<sup>†#</sup> Feier Li,<sup>†</sup> Chongxiong Duan,<sup>†\*</sup> and Hongxia Xi<sup>‡,\*</sup>*

<sup>†</sup>School of Chemistry and Chemical Engineering, South China University of Technology, Guangzhou 510640, PR China.

<sup>‡</sup>Guangdong Provincial Key Laboratory of Atmospheric Environment and Pollution Control, Guangzhou Higher Education Mega Centre, Guangzhou 510006, P. R. China.

### Table of Contents

<b>Experimental section</b> .....	S3
Chemical reagents .....	S3
Synthesis of conventional Cu-BTC using solvothermal method at 120 °C.....	S3
Control experiment 1: Synthesis of hierarchical porous Cu-BTC using solvothermal method	S4
Control experiment 2: Synthesis of Cu-BTC with sodium benzene sulfonate as template at room temperature and pressure.....	S5
Control experiment 3: Synthesis of Cu-BTC with HDS at room temperature and pressure.....	S5
Synthesis of a series of hierarchically porous Cu-BTC using other anionic surfactant as templates at room temperature and pressure .....	S5
In Situ Time-Resolved ATR-FTIR for hierarchical porous Cu-BTC growth.....	S5

Catalyze the Henry reaction .....	S5
<b>Materials characterization</b> .....	S6
<b>Calculation</b> .....	S7
<b>Calculation of STYs</b> .....	S7
<b>Computational study</b> .....	S7
<b>Table S1</b> .....	S8
<b>Table S2</b> .....	S8
<b>Table S3</b> .....	S9
<b>Figure S1</b> .....	S9
<b>Figure S2</b> .....	S9
<b>Figure S3</b> .....	S10
<b>Figure S4</b> .....	S10
<b>Figure S5</b> .....	S10
<b>Figure S6</b> .....	S11
<b>Figure S7</b> .....	S11
<b>Figure S8</b> .....	S11
<b>Figure S9</b> .....	S12
<b>Figure S10</b> .....	S12
<b>Figure S11</b> .....	S12
<b>Figure S12</b> .....	S13
<b>Figure S13</b> .....	S13

Figure S14 .....S13

Figure S15 .....S14

Figure S16 .....S14

## 1. Experimental section

**1.1 Chemical reagents:** Zinc oxide (ZnO, 99%), copper(II) nitrate trihydrate ( $\text{Cu}(\text{NO}_3)_2 \cdot 3\text{H}_2\text{O}$ , 99%), 1, 3, 5-benzenetricarboxylic acid ( $\text{H}_3\text{BTC}$ , 99%), sodium benzene sulfonate (SBS,  $\text{C}_6\text{H}_5\text{NaO}_3\text{S}$ ), sodium 4-hydroxybenzenesulfonatesodium dehydrate ( $\text{C}_6\text{H}_5\text{NaO}_4\text{S} \cdot 2\text{H}_2\text{O}$ , 98%), sodium *p*-toluenesulfonate ( $\text{C}_7\text{H}_8\text{NaO}_3\text{S}$ , 98%), sodium dodecyl benzene sulphonate ( $\text{C}_{18}\text{H}_{29}\text{NaO}_3\text{S}$ , 95%), nitromethane ( $\text{CH}_3\text{NO}_2$ , 99.0%), ethyl acetate ( $\text{CH}_3\text{COOC}_2\text{H}_5$ , 99.5%), petroleum ether, 4-nitrobenzaldehyde ( $\text{C}_7\text{H}_5\text{NO}_3$ , 95%), *N,N*- dimethylformamide (DMF, 99.5%), and ethanol ( $\text{CH}_3\text{CH}_2\text{OH}$ , 99.7%) were purchased from J&K Chemical Ltd. All of above chemical reagents were used without further purification.

### 1.2 Synthesis of conventional Cu-BTC using solvothermal method at 120 °C

In a typical synthesis,<sup>1</sup> 4.5 mmol of  $\text{Cu}(\text{NO}_3)_2 \cdot 3\text{H}_2\text{O}$  was added to 15 mL of deionized water to obtain solution A. 2.5 mmol of  $\text{H}_3\text{BTC}$  was added to 15 mL of ethanol to obtain solution B. After stirring for 30 min, solution A was added to solution B and the mixture was stirred for 30 min. The final gel mixture was transferred into a 100 mL Teflon-lined stainless steel autoclave stewing and heated to 120 °C for 12 h. After cooling down to room temperature, the solid product was filtered and washed with ethanol for 4 times. The final product was dried at 120 °C for 12 h and denoted as C-Cu-BTC.

### **1.3 Control experiment 1: Synthesis of hierarchically porous Cu-BTC using solvothermal method**

4.5 mmol of  $\text{Cu}(\text{NO}_3)_2 \cdot 3\text{H}_2\text{O}$  was added to 15 mL of deionized water as solution A. 2.5 mmol of  $\text{H}_3\text{BTC}$  and 2.25 mmol of SBS surfactant were added to 15 mL of ethanol as solution B. After stirring for 30 min, solution A was added to solution B and the mixture was stirred for 30 min more. The final gel mixture was transferred into a 100 mL Teflon-lined stainless steel autoclave stewing and heated to 120 °C for 12 h. After cooling down, the solid product was filtered and washed with ethanol for four times. The resulting product was dried at 120 °C for 12 h and denoted as Cu-BTC\_S.

### **1.4 Control experiment 2: Synthesis of Cu-BTC with SBS as template at room temperature and pressure**

4.5 mmol of  $\text{Cu}(\text{NO}_3)_2 \cdot 3\text{H}_2\text{O}$  was added to 15 mL of deionized water to obtain solution A. 2.5 mmol of  $\text{H}_3\text{BTC}$  and 2.25 mmol of SBS surfactant were added to 15 mL of ethanol to obtain solution B. After stirring for 30 min, solution A was added to solution B and the mixture was stirred for 60 s.

### **1.5 Control experiment 3: Synthesis of Cu-BTC with HDS at room temperature and pressure**

In a typical synthesis,<sup>2</sup> 0.293 g of ZnO was dispersed in 8 mL of  $\text{H}_2\text{O}$  and 8 mL of DMF using sonication for 30 min to form the suspension A. 4.5 mmol of  $\text{Cu}(\text{NO}_3)_2 \cdot 3\text{H}_2\text{O}$  was added to 15 mL of deionized water to obtain solution B. Then, 2.5 mmol of  $\text{H}_3\text{BTC}$  was added to 15 mL of ethanol to obtain solution C. Solution B was added to the solution

A to get (Cu, Zn) HDS and next the solution C were added under magnetic stirring. After reacting 60 s, the blue product was subsequently filtered and washed by methanol (25 mL, 4 times), then dried in an oven at 120 °C for 12 h. The resulting product is denoted as Cu-BTC\_H.

### **1.6 Synthesis of a series of hierarchically porous Cu-BTC using other surfactants as templates at room temperature and pressure**

The experimental procedures are similar to the above, except the SBS surfactant was replaced by sodium 4-hydroxybenzenesulfonate dehydrate, sodium *p*-toluenesulfonate, and sodium dodecyl benzene sulfonate, respectively. The resulting products are denoted as H-Cu-BTC\_Y2 ( $Y = B, C, D$ , where  $Y$  represents the type of surfactant, B: sodium 4-hydroxybenzenesulfonate dihydrate; C: sodium *p*-toluenesulfonate; D: sodium dodecyl benzene sulfonate; the molar ratio of surfactant/ $\text{Cu}^{2+} = 0.5$ ).

### **1.7 In situ time-resolved ATR-FTIR for hierarchically porous Cu-BTC growth**

ATR-FTIR spectroscopy (Mettler Toledo, ReactIR 15) was used to monitor the growth process of the HP-MOFs.<sup>3</sup> Specifically, in a typical synthesis, the ATR-FTIR infrared probe was placed in the mixture of  $\text{Cu}(\text{NO}_3)_2 \cdot 3\text{H}_2\text{O}$  and ZnO under fast magnetic stirring. Next, the prepared mixture of  $\text{H}_3\text{BTC}$  and SBS surfactant were added quickly to the (Cu, Zn) HDS mixture. Infrared absorbance spectra were recorded automatically every 15 s. Chemical information about the crystal growth was obtained from the changes in the infrared absorption peaks ( $\nu(\text{OCO}^-) \approx 1647 \text{ cm}^{-1}$ ,  $\nu(\text{C}=\text{C}) \approx 1588 \text{ cm}^{-1}$ , and  $\nu(\text{NO}_3) \approx 1360$  and  $1420 \text{ cm}^{-1}$ ).

## 1.8 Catalyze the Henry reaction

In a typical reaction,<sup>4</sup> 2.4 mL of nitromethane, 30 mg of 4-nitrobenzaldehyde, and 17.4 mg catalyst (H-Cu-BTC\_A2) were added into a Schlenk tube under magnetic stirring in nitrogen environment at 70 °C for 24 h. Then, the mixture was dissolved in ethyl acetate and evaporated by a rotary evaporator. The reactant and product were separate by chromatography method (the volume ratio of petroleum ether/ethyl acetate is 5:1). The crude product was dissolved in ethyl acetate and collected by evaporated.

## 2. Materials characterization

Powder X-ray diffraction (XRD) patterns of the samples were tested on Bruker D8 ADVANCE diffractometer system equipped with Ni filtered Cu target  $K\alpha$  radiation (40 kV, 40 mA, wave length  $\lambda = 0.15418$  nm) at room temperature. The simulated data were obtained from Materials Studio package 5.0. Fourier transform infrared (FTIR) spectra of the samples in the form of KBr pellets were examined on an FTIR spectrometer (Bruker Vector 33) with a resolution of  $4\text{ cm}^{-1}$ . Nitrogen adsorption-desorption isotherm was measured by ASAP 2020 (Micromeritics) system at 77 K. The specific surface areas of samples were calculated by the Brunauer-Emmett-Teller (BET) equation, and the pore size distribution was analyzed by density functional theory (DFT) method. T-plot micropore analysis was used to analyse the micropore volume ( $V_{\text{micro}}$ ) and the total pore volume ( $V_t$ ) was acquired by the single point adsorption branch of the isotherm. Scanning electron microscopy (SEM) images were examined on a Carl Zeiss, ZEISS Ultra 55 at a low landing energy (5.0 kV). Transmission electron microscopy (TEM)

were revealed on JEM- 2100HR electron microscope at 200kV. Thermogravimetric analysis (TGA) of the samples were tested on a TG 209 instrument (Netzsch) and heated from 298 to 873 K in N<sub>2</sub> atmosphere with a rate of 10 K/min. The growth process of products were monitored using *in-situ* infrared spectroscopy (ATR-FTIR, METTLER TOLEDO, ReactIR 15). The toluene adsorption experiment were performed on intelligent gravimetric analyzer (IGA-003).

### 3. Calculation

#### 3.1 Calculation of STYs

The space-time-yield (STY) can be calculated by the following Eq. (1)<sup>2</sup>

$$STY = \frac{m_{MOF}}{V_{solution} \cdot \tau} \times 1.44 \times 10^6 \quad (1)$$

Where  $m_{MOF}$  represents the powder mass (g) of HP-MOFs,  $V_{solution}$  represents the total volume (cm<sup>3</sup>) for mixture and  $\tau$  represents the stirring time (min).

#### 3.2 Mesodynamic (MesoDyn) simulation

Simulation parameters: to reproduce the chemical properties of the system during the mesodynamic (MesoDyn) simulations, a coarse-grained model is needed to represent the Gaussian chain of each repeating unit.<sup>5</sup> The molecules were simplified into one or more beads and all the beads had the same volume and mass. A bond between molecules was expressed by a spring with stretching behavior between beads.<sup>6</sup> Here, we chose the MOF precursor (H<sub>3</sub>BTC–Cu<sup>2+</sup>) and the template (C<sub>6</sub>H<sub>4</sub>NaSO<sub>3</sub>) as the objects to study. As shown in Figure S1, the coarse-grained model of C<sub>6</sub>H<sub>5</sub>NaSO<sub>3</sub> can be treated as a Gaussian chain with CS<sub>1</sub> topology, where one C bead represents a benzene segment and

one S bead represents a sodium sulfonate segment. In addition, the coarse-grained model of H<sub>3</sub>BTC–Cu<sup>2+</sup> (MOF precursor) can be treated as a benzene ring connected to three carboxyl groups. The carboxyl group and Cu<sup>2+</sup> were represented by O beads. In addition, the solvent molecules (ethanol and water) were represented by E and W beads, respectively. In the simulation system, the volume fractions of sodium benzene sulfonate, H<sub>3</sub>BTC–Cu<sup>2+</sup>, E beads, and W beads were 10%, 20%, 30%, and 40%, respectively.

The repulsion between beads was relative to the interaction energy between beads of like species. The value of the repulsion parameter can be derived from the Flory–Huggins parameter  $\chi$ .<sup>6</sup> Table S1 lists the  $\chi$  values between the beads used in this study. To simulate the mixing environment during the synthetic process, a constant shear effect was introduced into the simulation system after 0.25 ms. The *X*-axis is the velocity direction, the *Y*-axis is the velocity gradient direction, and the *Z*-axis is the neutral axis. The program achieved a stable shear, that is, the velocity gradient was uniform:  $d^2v_x/d^2v_y = \hat{U}_y$  and the shear rate  $\dot{\gamma} = 5 \times 10^5 \text{ s}^{-1}$ .<sup>7</sup> The simulated time step was  $\Delta\tau = 50 \text{ ns}$ , and the total simulation time was 1.0 ms (20000 steps in total).

**Table S1.** Flory-Huggins interaction parameter  $\chi$  between beads.

Bead	C	S	O	E	W
C	0	1.52	1.62	3.03	9.08
S			0.8	1.49	1.4
O			0	3.53	3.5
E				1.42	0.06
W					0

**Table S2.** Textural properties and STYs of the H-Cu-BTC\_XX ( $X = 1, 2, 3, 4$ ) and H-Cu-BTC\_Y2 ( $Y = B, C, D$ ) HP-MOFs.

Sample	Template /Cu <sup>2+</sup>	<sup>a</sup> S <sub>BET</sub> [m <sup>2</sup> ·g <sup>-1</sup> ]	<sup>b</sup> S <sub>meso</sub> / S <sub>micro</sub>	<sup>c</sup> V <sub>t</sub> [cm <sup>3</sup> ·g <sup>-1</sup> ]	<sup>d</sup> V <sub>micro</sub> [cm <sup>3</sup> ·g <sup>-1</sup> ]	<sup>e</sup> V <sub>meso</sub> [cm <sup>3</sup> ·g <sup>-1</sup> ]	<sup>f</sup> STY [kg·m <sup>-3</sup> ·d <sup>-1</sup> ]
H-Cu-BTC_A1	1:1	1262	0.22	0.67	0.48	0.19	1.96×10 <sup>4</sup>
H-Cu-BTC_A2	1:2	1156	0.20	0.64	0.49	0.15	2.90×10 <sup>4</sup>
H-Cu-BTC_A3	1:4	1529	0.22	0.75	0.58	0.17	2.32×10 <sup>4</sup>
H-Cu-BTC_A4	1:10	1548	0.21	0.77	0.59	0.18	1.94×10 <sup>4</sup>
H-Cu-BTC_B2	1:2	1504	0.13	0.62	0.51	0.11	2.36×10 <sup>4</sup>
H-Cu-BTC_C2	1:2	1154	0.15	0.51	0.39	0.12	2.15×10 <sup>4</sup>
H-Cu-BTC_D2	1:2	1397	0.14	0.59	0.47	0.12	2.57×10 <sup>4</sup>

<sup>a</sup>S<sub>BET</sub>: Brunauer–Emmett–Teller (BET) surface area; <sup>b</sup>S<sub>meso</sub>: mesopore BET surface area; <sup>b</sup>S<sub>micro</sub>: micropore BET surface area; <sup>c</sup>V<sub>t</sub>: total pore volume; <sup>d</sup>V<sub>micro</sub>: micropore volume; <sup>e</sup>V<sub>meso</sub>: mesopore volume; <sup>f</sup>STY: space–time yield, which was calculated based on the mass of active products.<sup>2</sup>

**Table S3.** Leaching test analysis of the recycling experiments.

Entry	Leaching of Cu* (ppm)
run 1	9.7
run 2	9.3
run 3	10.6

\*The leached Cu content was determined by inductively coupled plasma optical emission spectroscopy (Optima 5300DV).

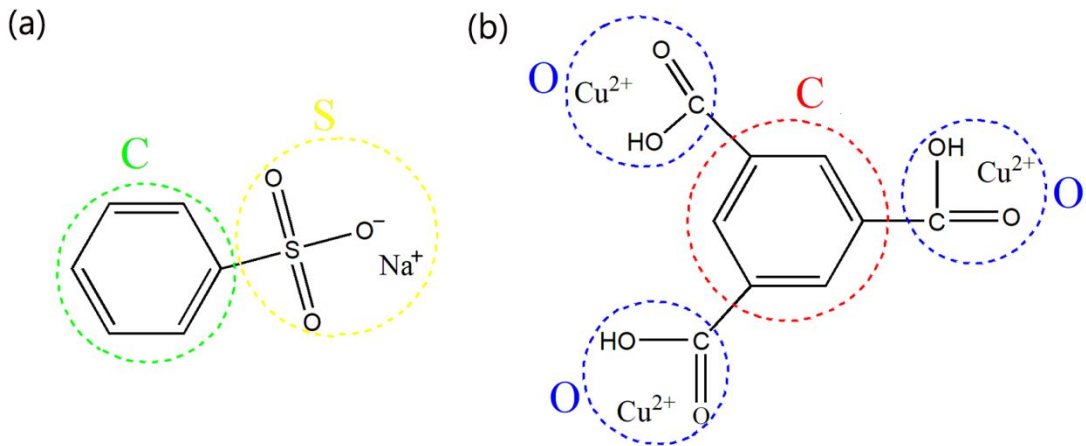


**Figure S1.** Coarse-grained model for the sodium benzene sulfonate and Cu-BTC precursor.

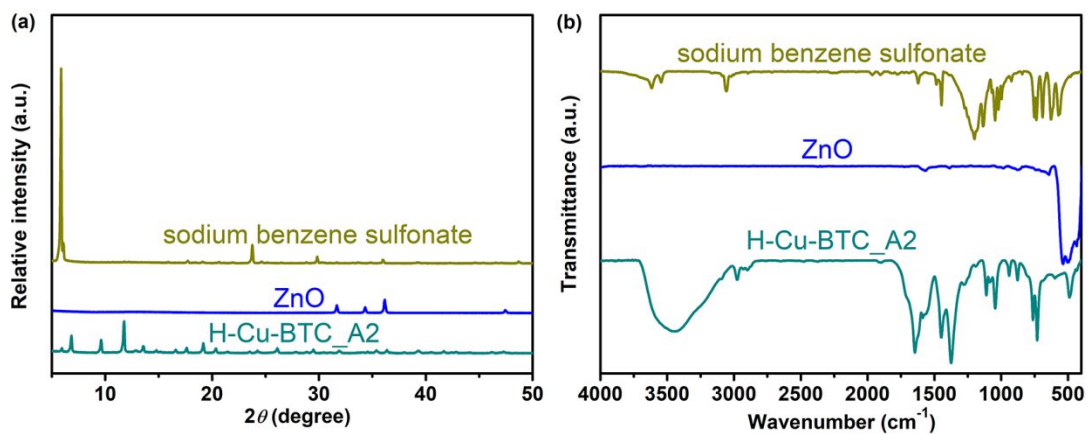


**Figure S2.** (a) Powder XRD patterns and (b) FTIR spectra of H-Cu-BTC\_A2, ZnO, and SBS surfactant.

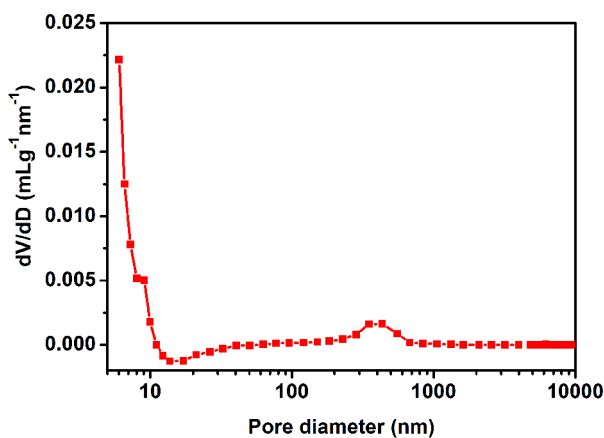


**Figure S3.** Pore size distribution of H-Cu-BTC\_A2 measured by mercury intrusion porosimetry.

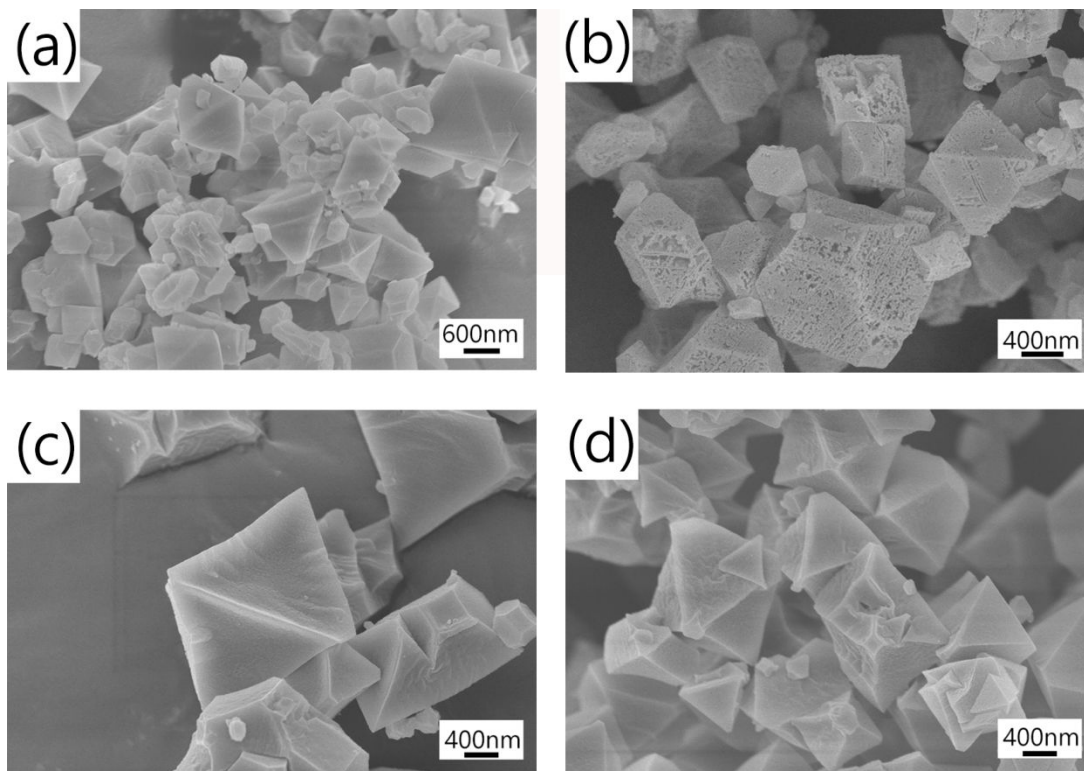


**Figure S4.** SEM images of H-Cu-BTC<sub>AX</sub>: (a) H-Cu-BTC<sub>A1</sub>, (b) H-Cu-BTC<sub>A2</sub>, (c) H-Cu-BTC<sub>A3</sub>, and (d) H-Cu-BTC<sub>A4</sub>.

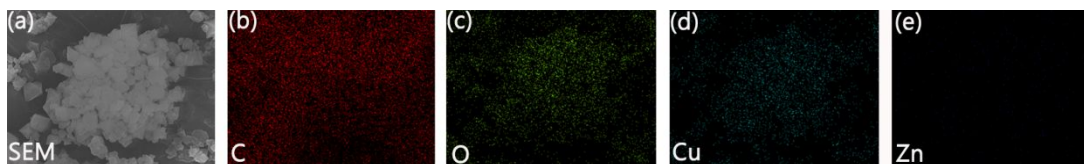


**Figure S5.** Elemental distribution maps of H-Cu-BTC<sub>A2</sub> sample: (a) the selected crystal, (b) C, (c) O, (d) Cu, and (e) Zn.

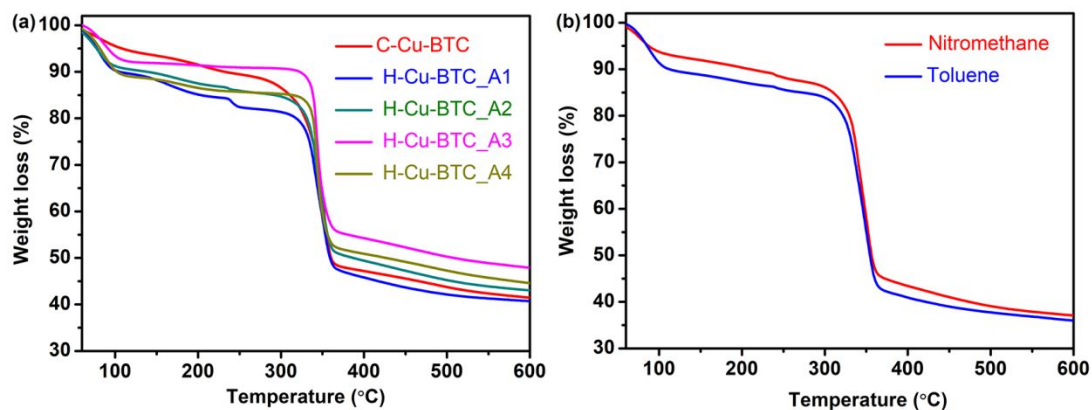


**Figure S6.** (a) Thermogravimetric analysis (TGA) curves of H-Cu-BTC<sub>AX</sub> ( $X = 1, 2, 3, 4$ ) and C-Cu-BTC, and (b) TGA curves of H-Cu-BTC<sub>A2</sub> after immersion in nitromethane and toluene for 3 days under ambient conditions.

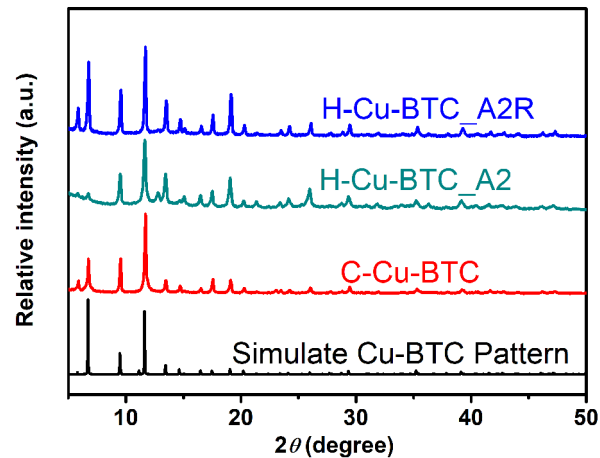


**Figure S7.** Powder XRD patterns of H-Cu-BTC\_A2R, H-Cu-BTC\_A2, and C-Cu-BTC, and the simulated pattern for single-crystal Cu-BTC.

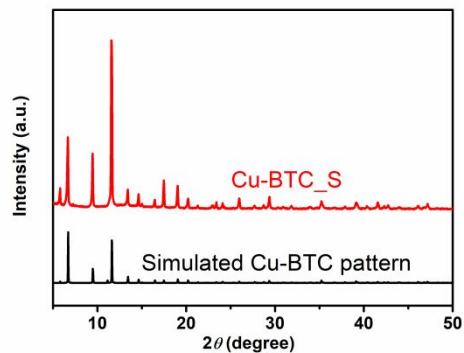


**Figure S8.** Powder XRD patterns of Cu-BTC\_S and the simulated pattern for single-crystal Cu-BTC.

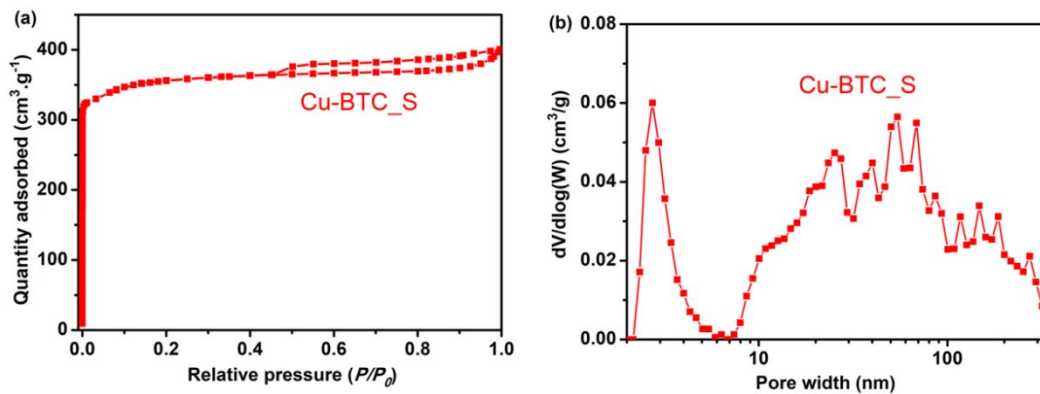


**Figure S9.** (a) N<sub>2</sub> adsorption–desorption isotherms and (b) pore size distributions of Cu-BTC\_S sample.

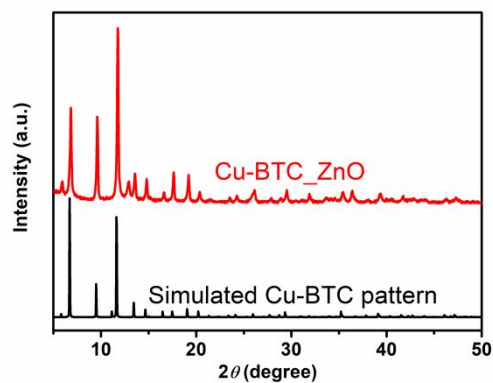


**Figure S10.** Powder XRD patterns of Cu-BTC\_ ZnO and the simulated pattern for single-crystal Cu-BTC.

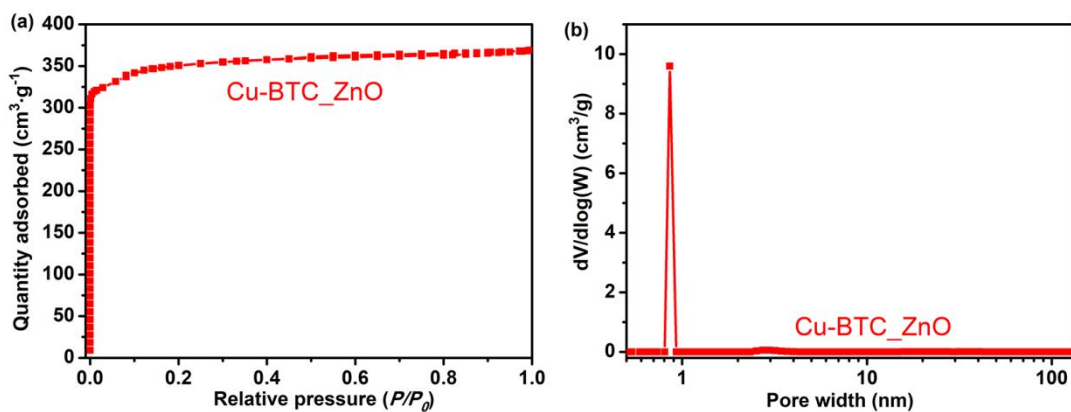


**Figure S11.** (a) N<sub>2</sub> adsorption–desorption isotherms and (b) pore size distributions of the Cu-BTC\_ ZnO.

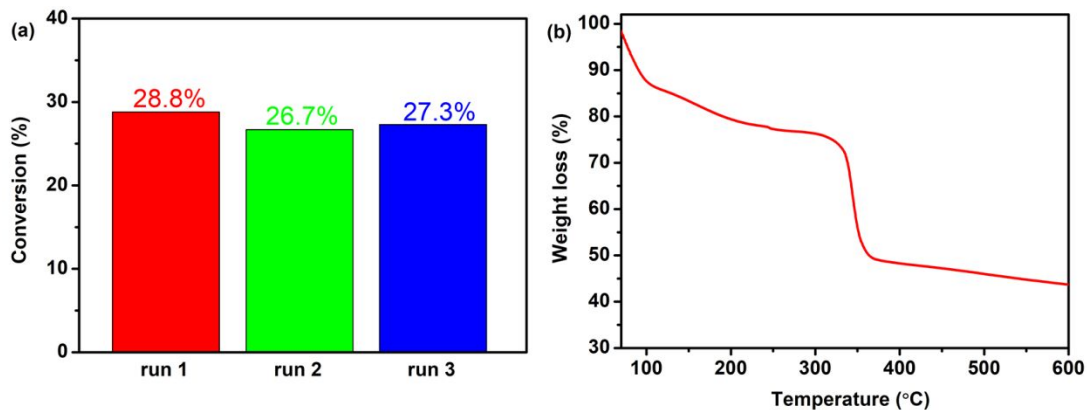


**Figure S12.** (a) Conversion as a function of the number of recycle runs using H-Cu-BTC\_A2 as the catalyst; and (b) TGA of the H-Cu-BTC\_A2 after catalytic cycles.

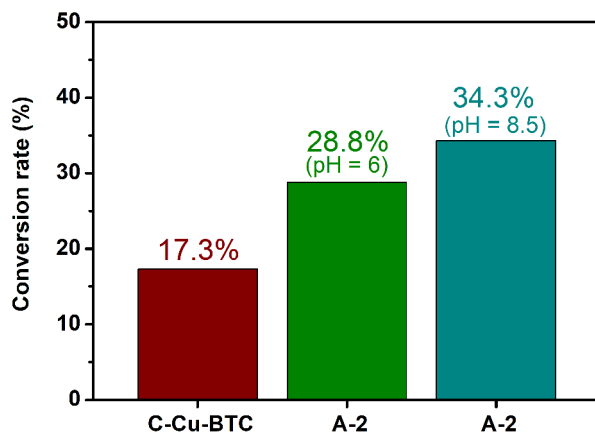


**Figure S13.** Conversion rate of 4-nitrobenzaldehyde catalyzed by A-2 (H-Cu-BTC\_A2) at different catalytic system.

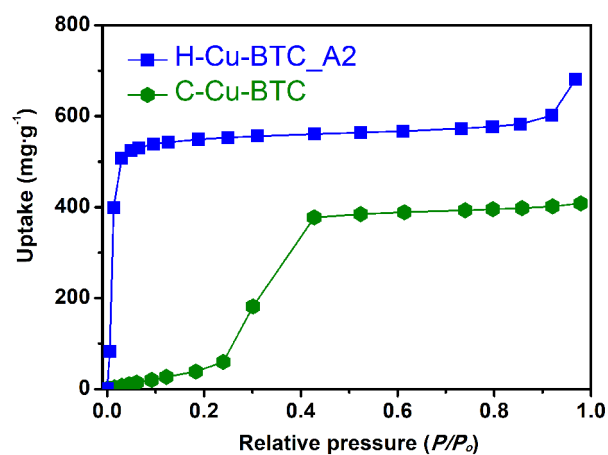


**Figure S14.** Toluene sorption isotherms at 298K on C-Cu-BTC and H-Cu-BTC\_A2 samples, respectively.

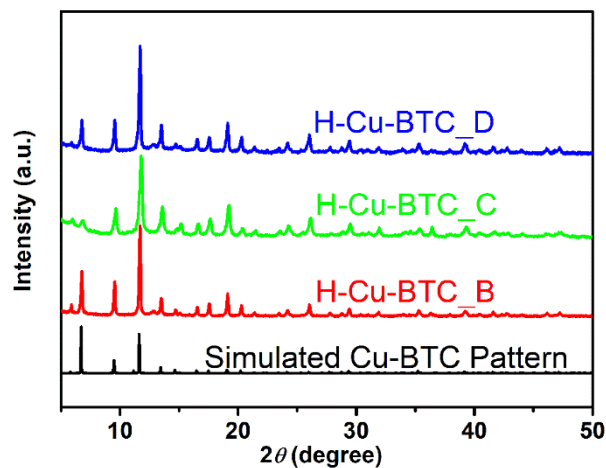


**Figure S15.** Powder XRD patterns of H-Cu-BTC\_Y2 (Y = B, C, D) and the simulated pattern.

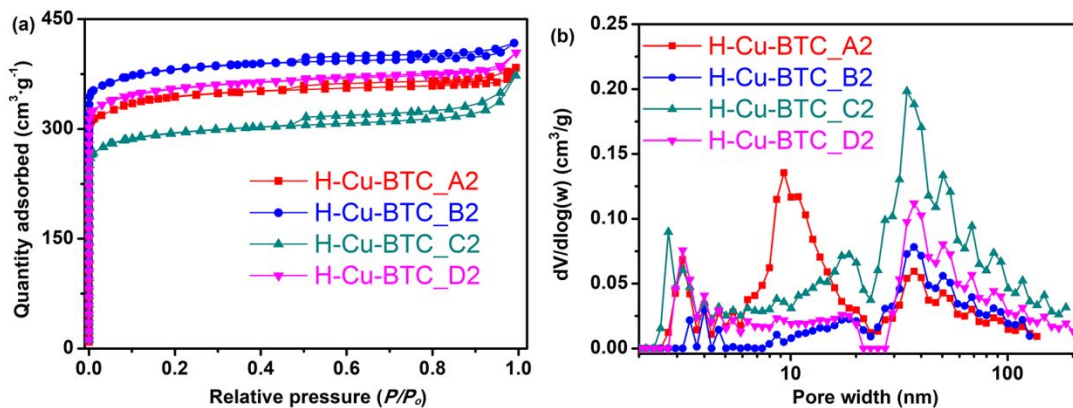


**Figure S16.** (a) N<sub>2</sub> adsorption–desorption isotherms and (b) pore size distributions of the H-Cu-BTC\_A2 and H-Cu-BTC\_Y2 (Y = B, C, D).

## References

- (1) Duan, C.; Li, F.; Zhang, H.; Li, J.; Wang, X.; Xi, H. Template synthesis of hierarchical porous metal-organic frameworks with tunable porosity. *RSC Adv.* **2017**, *7*, 52245-52251.
- (2) Zhao, J.; Nunn, W. T.; Lemaire, P. C.; Lin, Y.; Dickey, M. D.; Oldham, C. J.; Walls, H. J.; Peterson, G. W.; Losego, M. D.; Parsons, G. N. Facile Conversion of Hydroxy Double Salts to Metal-Organic Frameworks Using Metal Oxide Particles and Atomic Layer Deposition Thin-Film Templates. *J. Am. Chem. Soc.* **2015**, *137*, 13756-13759.
- (3) Zhao, J.; Kalanyan, B.; Barton, H. F.; Sperling, B. A.; Parsons, G. N. In Situ Time-Resolved Attenuated Total Reflectance Infrared Spectroscopy for Probing Metal–Organic Framework Thin Film Growth. *Chem. Mater.* **2017**, *29*, 8804-8810.
- (4) Duan, C.; Li, F.; Luo, S.; Xiao, J.; Li, L.; Xi, H. Facile synthesis of hierarchical porous metal-organic frameworks with enhanced catalytic activity. *Chem. Eng. J.* **2018**, *334*, 1477-1483.
- (5) Li, Y.-m.; Xu, G.-y.; Wu, D.; Sui, W.-p. The aggregation behavior between anionic carboxymethylchitosan and cetyltrimethylammonium bromide: MesoDyn simulation and experiments. *Eur. Polym. J.* **2007**, *43*, 2690-2698.
- (6) Zhao, X.; Wang, Z.; Yuan, S.; Lu, J.; Wang, Z. MesoDyn prediction of a pharmaceutical microemulsion self-assembly consistent with experimental measurements. *RSC Adv.* **2017**, *7*, 20293-20299.
- (7) Chen, H.; Wu, Y.; Tan, Y.; Li, X.; Qian, Y.; Xi, H. Mesoscopic simulation of surfactant/silicate self-assembly in the mesophase formation of SBA-15 under charge matching interactions. *Eur. Polym. J.* **2012**, *48*, 1892-1900.